



Observation of new baryons in the $\Xi_b^- \pi^+ \pi^-$ and $\Xi_b^0 \pi^+ \pi^-$ systems

LHCb collaboration[†]

Abstract

The first observation and study of two new baryonic structures in the final state $\Xi_b^0 \pi^+ \pi^-$ and the confirmation of the $\Xi_b(6100)^-$ state in the $\Xi_b^- \pi^+ \pi^-$ decay mode are reported using proton-proton collision data collected by the LHCb experiment, corresponding to an integrated luminosity of 9 fb^{-1} . In addition, the properties of the known Ξ_b^{*0} , $\Xi_b'^-$ and Ξ_b^{*-} resonances are measured with improved precision. The new decay mode of the Ξ_b^0 baryon to the $\Xi_c^+ \pi^- \pi^+ \pi^-$ final state is observed and exploited for the first time in these measurements.

Published in Phys. Rev. Lett. 131 (2023) 171901

© 2024 CERN for the benefit of the LHCb collaboration. CC BY 4.0 licence.

[†]Authors are listed at the end of this Letter.

The $\Xi_b^{(-,0)}$ baryons form an isospin doublet and are made of a b quark, an s quark and a lighter q (u or d) quark. Their ground states have angular momentum $L = 0$ between the b quark and the light diquark. Three isospin doublets of such non-excited states are expected in the quark model [1–3] with different spin-parity J^P and angular momentum of the sq diquark J_{sq} . The $\Xi_b^{(-,0)}$, $\Xi_b^{\prime(0,-)}$ and $\Xi_b^{*(0,-)}$ states are characterized by (J_{sq}, J^P) values of $(0, \frac{1}{2}^+)$, $(1, \frac{1}{2}^+)$ and $(1, \frac{3}{2}^+)$, respectively. Although five of these states have been observed experimentally [4–7], the $\Xi_b^{\prime 0}$ baryon remains unobserved. This may be because its mass lies below the threshold for the $\Xi_b^{\prime 0} \rightarrow \Xi_b^- \pi^+$ decay [8, 9], meaning that it only decays to either the $\Xi_b^0 \pi^0$ or $\Xi_b^0 \gamma$ final states making it experimentally challenging to observe. A number of excited states of higher mass is expected, with predictions for their properties available, *e.g.* in Refs. [9–17]. The CMS collaboration has reported the observation of the $\Xi_b(6100)^-$ resonance in the $\Xi_b^- \pi^+ \pi^-$ final state, using Ξ_b^- decays to final states containing J/ψ mesons [18].

In this Letter, both the $\Xi_b^- \pi^+ \pi^-$ and $\Xi_b^0 \pi^+ \pi^-$ final states and their intermediate $\Xi_b^- \pi^+$ and $\Xi_b^0 \pi^-$ states are investigated experimentally (the inclusion of charge conjugate processes and the use of natural units are implicit throughout this Letter), using pp collision data collected by the LHCb experiment at centre-of-mass energies of 7, 8, 13 TeV, corresponding to an integrated luminosity of 9 fb^{-1} . The observation of three narrow states is reported and their properties are measured.

The LHCb detector [19, 20] is a single-arm forward spectrometer covering the pseudorapidity range $2 < \eta < 5$. The detector includes a high-precision tracking system consisting of a silicon-strip vertex detector surrounding the pp interaction region [21], a large-area silicon-strip detector located upstream of a dipole magnet with a bending power of about 4 Tm, and three stations of silicon-strip detectors and straw drift tubes [22, 23] placed downstream of the magnet. Different types of charged hadrons are distinguished using information from two ring-imaging Cherenkov detectors [24]. Simulated data samples are produced with the software packages described in Refs. [25–29] and are used to model the detector resolution and optimize the selection criteria.

Samples of Ξ_b^- (Ξ_b^0) candidates are formed from $\Xi_c^0 \pi^-$ ($\Xi_c^+ \pi^-$) and $\Xi_c^0 \pi^- \pi^+ \pi^-$ ($\Xi_c^+ \pi^- \pi^+ \pi^-$) combinations, where the Ξ_c^0 (Ξ_c^+) baryon is reconstructed in the $pK^-K^- \pi^+$ ($pK^- \pi^+$) final state. To suppress background coming from promptly produced particles, all $\Xi_b^{(-,0)}$ decay products are required to be displaced significantly from all primary pp collision vertices (PVs) in the event. The reconstructed Ξ_c^0 (Ξ_c^+) candidates are required to have a mass within 20 MeV (25 MeV) of the respective world-average mass values [30]. Displaced pion tracks are combined with Ξ_c candidates to form $\Xi_b^{(-,0)}$ candidates, requiring good vertex-fit quality and significant displacement of the $\Xi_b^{(-,0)}$ decay point from any PV in the event. All charged particles are required to have particle-identification (PID) information consistent with their respective mass hypotheses. PID variables are based on neural network algorithms [31] and their distributions in simulation are calibrated using data [32]. If multiple candidates per collision event pass the selection requirements, all of them are preserved in the data sample. The topological, kinematic and PID variables are used as inputs to a Boosted Decision Tree (BDT) classifier [33] that discriminates $\Xi_b^{(-,0)}$ signal candidates from random track combinations. The classifier is trained using simulated $\Xi_b^{(-,0)}$ decays as a signal proxy and $\Xi_b^{(-,0)}$ data candidates in the sideband $5900 < m(\Xi_c^{(0,+)} \pi^-, \Xi_c^{(0,+)} \pi^- \pi^+ \pi^-) < 6000$ MeV as a background proxy. The mass distributions of the selected $\Xi_b^{(-,0)} \rightarrow \Xi_c^{(0,+)} \pi^-$ and $\Xi_b^{(-,0)} \rightarrow \Xi_c^{(0,+)} \pi^- \pi^+ \pi^-$ candidates are

shown in the supplemental material [34]. The decay mode $\Xi_b^0 \rightarrow \Xi_c^+ \pi^- \pi^+ \pi^-$ is observed for the first time experimentally. The selection requirement on the BDT classifier output is optimized for the observation of new states and retains 96% of the Ξ_b^- and 92% of the Ξ_b^0 signal candidates. Additional vetoes are imposed, as described in Ref. [35], to suppress other abundant processes with displaced vertices *e.g.* those coming from D^0 , D^+ , D_s^+ and Λ_c^+ decays with a misidentified particle.

The $\Xi_b^{(-,0)}$ candidates within a ± 75 MeV window around the peak position are combined with one charged pion (two pions) to investigate the $\Xi_b^- \pi^+$ and $\Xi_b^0 \pi^-$ ($\Xi_b^- \pi^+ \pi^-$ and $\Xi_b^0 \pi^- \pi^+$) mass spectra. In order to improve the mass resolution, the obtained candidates are refitted with the masses of the $\Xi_b^{(-,0)}$ and $\Xi_c^{(0,+)}$ baryon candidates constrained to their known values [30] and the $\Xi_b^{(-,0)}$ flight direction to originate from the PV [36]. Additional requirements are applied to the $\Xi_b \pi^- \pi^+$ candidates, where the Ξ_b^{*0} , $\Xi_b'^-$ and Ξ_b^{*-} intermediate states are selected according to their observed widths and known mass values [30]. Signal mass windows for the $\Xi_b \pi$ intermediate resonances are defined as $|m(\Xi_b \pi) - m_{\Xi_b^{*0}}| < 3$ MeV, $|m(\Xi_b \pi) - m_{\Xi_b'^-}| < 1.25$ MeV and $|m(\Xi_b \pi) - m_{\Xi_b^{*-}}| < 5$ MeV, each corresponding to 2.5σ of the observed experimental peak.

The signal yields and lineshape parameters of the signal resonances are determined with an extended unbinned maximum-likelihood fit to the Q -value distributions defined as $m_{\Xi_b \pi} - m_{\Xi_b} - m_\pi$ and $m_{\Xi_b \pi \pi} - m_{\Xi_b} - 2m_\pi$ for $\Xi_b \pi$ and $\Xi_b \pi \pi$ decays, respectively. The mass distributions of the $\Xi_b^- \pi^+$ and $\Xi_b^0 \pi^-$ ($\Xi_b^- \pi^+ \pi^-$ and $\Xi_b^0 \pi^- \pi^+$) samples are shown in Fig. 1 (Fig. 2), together with the results of the fit. All signal components are modeled using relativistic Breit–Wigner distributions [37] including Blatt–Weisskopf form factors [38] with a radius of 3 GeV^{-1} . The orbital angular momentum between the $\Xi_b^{(-,0)}$ baryons and the pions is assumed according to the expected spin assignment. The relativistic Breit–Wigner distributions are convolved with functions parameterizing the detector resolution. These resolution models are determined from simulation samples and are consistent with a resolution that scales as \sqrt{Q} . Simulation shows that for each resonance, the resolution is comparable to or smaller than the measured natural widths of the peaks, with the exception of the $\Xi_b'^-$ baryon. The background contribution is parameterized as $(Q - d)^n$, where d and n parameters vary freely in the fit. This function, which is validated using wrong-charge $\Xi_b^- \pi^-$ and $\Xi_b^0 \pi^+$ candidates, is sufficient to describe the smooth background coming from random track combinations. Additional components are included in the fit to the $\Xi_b^0 \pi^-$ spectrum to describe partially reconstructed candidates coming from higher mass resonances. These components are referred to as *reflections* in the rest of this Letter. The reflections of the newly observed states in the $\Xi_b \pi \pi$ mode to the $\Xi_b \pi$ spectrum are studied with simulation and dedicated components are included in the fit, modeled as Gaussian functions with power-law tails [39]. The means of the reflection components vary freely in the fits to data and their fitted values are consistent with expectations from simulated backgrounds and cross-checks in data. The fit confirms the presence of partially reconstructed $\Xi_b(6100)^- \rightarrow \Xi_b^{*0}(\Xi_b^0 \pi^0) \pi^-$ decays and shows hints of a contribution from the decay chain $\Xi_b(1P, 1/2)^- \rightarrow \Xi_b'^0(\Xi_b^0 \pi^0) \pi^-$, where neither the $\Xi_b(1P, 1/2)^-$ state, the expected lighter resonance equivalent to that found in the neutral system, nor the $\Xi_b'^0$ state has been observed experimentally to date (Fig. 2). This component has been validated simulating different mass and width hypotheses for the two particles involved, taking into account expected isospin splittings given the masses of their charged partners. However, a precise estimation of the $\Xi_b(1P, 1/2)^-$ and $\Xi_b'^0$ state

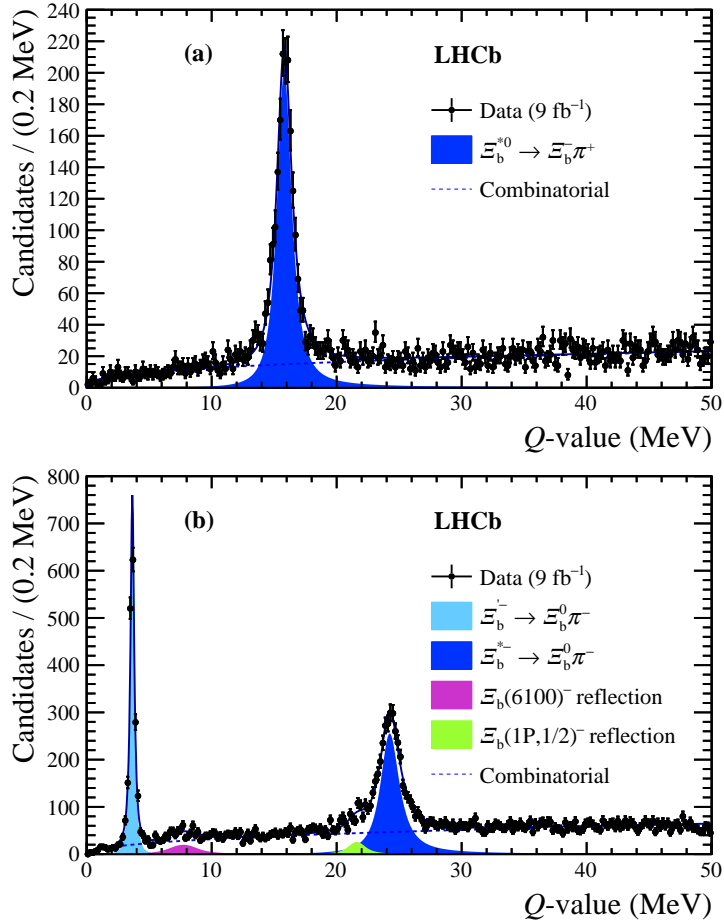


Figure 1: Distributions of the mass difference $Q = m_{\Xi_b \pi} - m_{\Xi_b} - m_\pi$ for selected (a) $\Xi_b^- \pi^+$ and (b) $\Xi_b^0 \pi^-$ candidates. The fit results are superimposed.

properties is not possible due to the limited yield and the presence of two unknown mass values. The resolutions of the signal components are fixed to the values obtained from simulation. The fit models are validated with pseudoexperiments and no significant bias is found on any of the parameters of interest.

The fitted yields in the $\Xi_b \pi$ mass spectra are 2019 ± 58 for the Ξ_b^{*0} baryon, 1750 ± 50 for the $\Xi_b'^-$ baryon and 3380 ± 110 for the Ξ_b^{*-} baryon. The $\Xi_b(6100)^-$ state [18] is confirmed in the $\Xi_b^{*0} \pi^-$ mass distribution (Fig. 2a), while two new peaks are observed in the $\Xi_b'^- \pi^+$ (Fig. 2b) and $\Xi_b^{*-} \pi^+$ (Fig. 2c) mass distributions, referred to as $\Xi_b(6087)^0$ and $\Xi_b(6095)^0$ in this Letter. For the newly observed states, the signal yields are 136 ± 17 for the $\Xi_b(6100)^-$ resonance, 147 ± 19 for the $\Xi_b(6087)^0$ resonance and 69 ± 14 for the $\Xi_b(6095)^0$ resonance. The three peaks are observed with local significances of 18σ , 15σ and 9σ , based on the differences in log-likelihood between a fit with the signal yield fixed to zero and the default fit. These significances are reduced to 12σ , 10σ and 8σ , once systematic uncertainties on the yields are taken into account.

Different sources of systematic uncertainties are considered in the determination of the resonance parameters. All these systematic uncertainties are summarized in Table 1. One of the most important contributions to the mass measurements comes from the knowledge of the momentum scale at LHCb. The associated systematic uncertainty is assigned as the

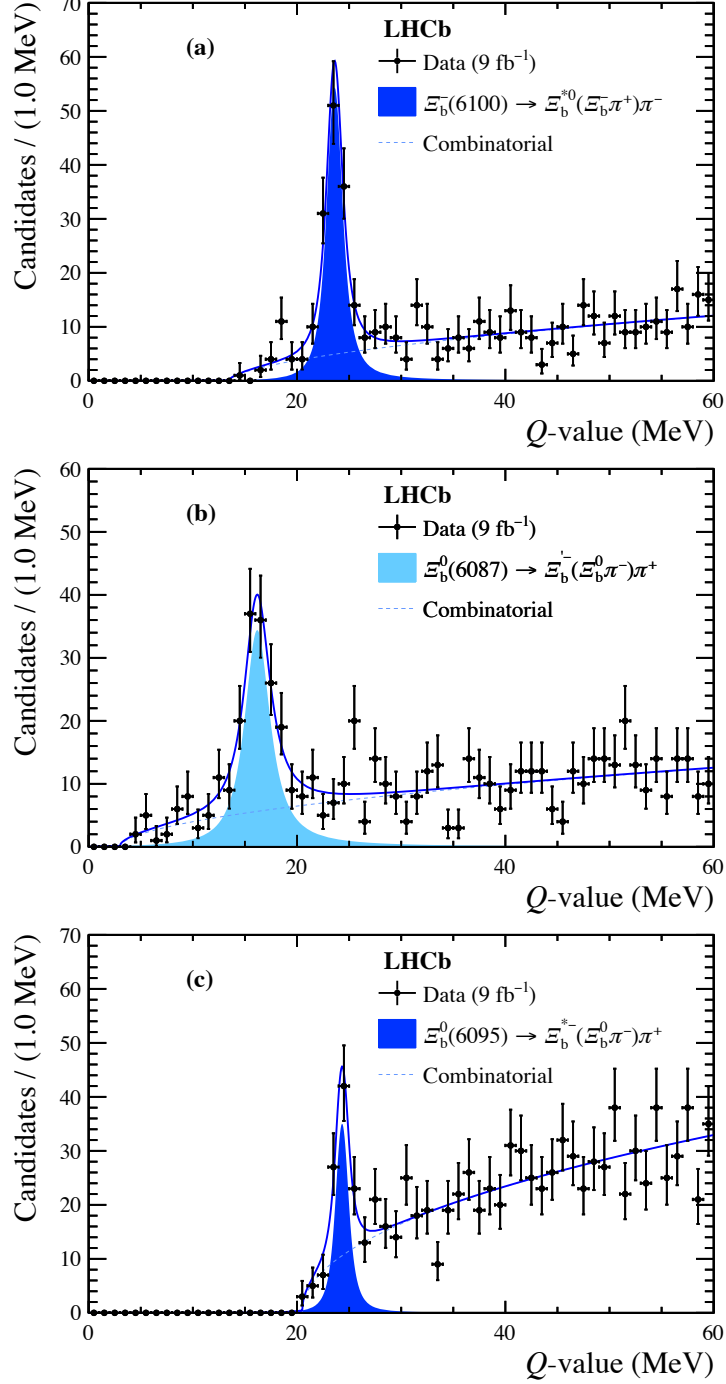


Figure 2: Distributions of the mass difference $Q = m_{\Xi_b \pi \pi} - m_{\Xi_b} - 2m_\pi$ for selected (a) $\Xi_b^{*-} \pi^+ \pi^-$ candidates in the Ξ_b^{*0} mass window, (b) $\Xi_b^0 \pi^- \pi^+$ candidates in the Ξ_b^0 mass window and (c) $\Xi_b^0 \pi^- \pi^+$ candidates in the Ξ_b^{*-} mass window. The fit results are superimposed.

larger of the changes in the measured parameters when the momentum scale is changed by its uncertainty, which is estimated to be 3×10^{-4} [40]. An additional uncertainty arises from the empirical description of the background shapes and is estimated by modeling them with alternative functions. A third uncertainty is assigned by varying the description of the reflection components and their properties, obtained either from simulation or

Table 1: Systematic uncertainties (MeV) on the measured physical properties. The parameters Q_0 and Γ are the mean and the width of the Breit–Wigner distribution, respectively.

| Source | Ξ_b^{*0} | | $\Xi_b^{\prime-}$ | | Ξ_b^{*-} | |
|----------------|--------------|----------|-------------------|----------|--------------|----------|
| | Q_0 | Γ | Q_0 | Γ | Q_0 | Γ |
| Momentum scale | 0.006 | 0.001 | 0.001 | 0.001 | 0.008 | 0.001 |
| Background | 0.003 | 0.029 | 0.000 | 0.006 | 0.004 | 0.073 |
| Reflections | | | 0.000 | 0.000 | 0.002 | 0.007 |
| Resolution | 0.001 | 0.038 | 0.002 | 0.027 | 0.000 | 0.033 |
| BW param. | 0.001 | 0.001 | 0.000 | 0.000 | 0.001 | 0.002 |
| Total | 0.007 | 0.048 | 0.002 | 0.028 | 0.010 | 0.081 |

| Source | $\Xi_b(6100)^-$ | | $\Xi_b(6087)^0$ | | $\Xi_b(6095)^0$ | |
|----------------|-----------------|----------|-----------------|----------|-----------------|----------|
| | Q_0 | Γ | Q_0 | Γ | Q_0 | Γ |
| Momentum scale | 0.008 | 0.002 | 0.007 | 0.001 | 0.009 | 0.006 |
| Background | 0.004 | 0.035 | 0.022 | 0.089 | 0.023 | 0.025 |
| Resolution | 0.004 | 0.054 | 0.001 | 0.035 | 0.006 | 0.073 |
| BW param. | 0.016 | 0.050 | 0.056 | 0.007 | 0.001 | 0.079 |
| Total | 0.019 | 0.081 | 0.060 | 0.096 | 0.026 | 0.111 |

from data, where relevant. Further sources of uncertainty on the measurement of the natural widths are included to describe the known differences in resolution between data and simulated events. Differences are expected to be within 5%, based on previous studies [41–44], therefore uncertainties are estimated by varying the resolution function width and the parametrization of the mass resolution function by that amount. Possible uncertainties can arise from the assumed relativistic Breit–Wigner distributions and their parameters. Lower mass states are assumed to decay with angular momentum $l = 0$, while higher mass states with $l = 1$. For the newly observed states, the hypotheses assuming $l = 0, 2, 3$ are tested and the largest shifts of the fitted parameters with respect to the default fit are assigned as systematic uncertainties. A further uncertainty on the baryon mass m_0 is assigned due to the limited knowledge of the Ξ_b^- and Ξ_b^0 baryon masses [30].

The numerical results are summarized in Table 2. The properties of the Ξ_b^{*0} , $\Xi_b^{\prime-}$ and Ξ_b^{*-} baryons are measured with world-leading precision. For the narrow $\Xi_b^{\prime-}$ state, its natural width is compatible with zero once the systematic uncertainties are considered, and an upper limit < 0.05 MeV is estimated at 90% confidence level.

In summary, the first observation of two new baryons $\Xi_b(6087)^0$ and $\Xi_b(6095)^0$, with quark content bsu , is reported in the $\Xi_b^0 \pi^+ \pi^-$ final state. Additionally, this Letter confirms the observation of the $\Xi_b(6100)^-$ charged state by the CMS collaboration [18], with improved significance and sensitivity on its physical parameters. This measurement uses final states with up to nine tracks, most of which are pions, showing excellent performance of the LHCb tracking, reconstruction and PID systems. Finally, the decay mode $\Xi_b^0 \rightarrow \Xi_c^+ \pi^- \pi^+ \pi^-$ is observed for the first time. The properties of the Ξ_b^{*0} , $\Xi_b^{\prime-}$ and Ξ_b^{*-} baryons are measured with high precision. Determination of the spin and parity for the new baryons is not possible given the low signal yields. However, data indicate that the $\Xi_b(6100)^-$ baryon decays mainly through the $\Xi_b^{*0} \pi^-$ state, the $\Xi_b(6087)^0$ baryon mainly through the $\Xi_b^{\prime-} \pi^+$ state, and the $\Xi_b(6095)^0$ baryon mainly through the $\Xi_b^{*-} \pi^+$ state, with no significant contributions to the signals from events outside their

Table 2: Masses and widths of the states considered in this Letter. The first uncertainty is statistical, the second systematic. The third uncertainty on m_0 is due to limited knowledge of the Ξ_b^- and Ξ_b^0 baryon masses [30].

| State | Observ. | Value (MeV) |
|-----------------|----------|---|
| $\Xi_b(6100)^-$ | Q_0 | $23.6 \pm 0.11 \pm 0.02$ |
| | Γ | $0.94 \pm 0.30 \pm 0.08$ |
| | m_0 | $6099.74 \pm 0.11 \pm 0.02 \pm 0.6$ (Ξ_b^-) |
| $\Xi_b(6087)^0$ | Q_0 | $16.20 \pm 0.20 \pm 0.06$ |
| | Γ | $2.43 \pm 0.51 \pm 0.10$ |
| | m_0 | $6087.24 \pm 0.20 \pm 0.06 \pm 0.5$ (Ξ_b^0) |
| $\Xi_b(6095)^0$ | Q_0 | $24.32 \pm 0.15 \pm 0.03$ |
| | Γ | $0.50 \pm 0.33 \pm 0.11$ |
| | m_0 | $6095.36 \pm 0.15 \pm 0.03 \pm 0.5$ (Ξ_b^0) |
| Ξ_b^{*0} | Q_0 | $15.80 \pm 0.02 \pm 0.01$ |
| | Γ | $0.87 \pm 0.06 \pm 0.05$ |
| | m_0 | $5952.37 \pm 0.02 \pm 0.01 \pm 0.6$ (Ξ_b^-) |
| $\Xi_b'^-$ | Q_0 | $3.66 \pm 0.01 \pm 0.00$ |
| | Γ | $0.03 \pm 0.01 \pm 0.03$ |
| | m_0 | $5935.13 \pm 0.01 \pm 0.00 \pm 0.5$ (Ξ_b^0) |
| Ξ_b^{*-} | Q_0 | $24.27 \pm 0.03 \pm 0.01$ |
| | Γ | $1.43 \pm 0.08 \pm 0.08$ |
| | m_0 | $5955.74 \pm 0.03 \pm 0.01 \pm 0.5$ (Ξ_b^0) |

respective $m_{\Xi_b\pi}$ mass windows [34]. These patterns closely resemble those observed in the Ξ_c^0 and Ξ_c^+ baryon systems [30]. An interpretation would be that the new states are P -wave states ($l = 1$ between the b quark and the qs diquark) coupling to the b quark to give a pair of states with $J^P = \frac{1}{2}^-$ and $\frac{3}{2}^-$. One might expect the dominant decay mode of the lighter one to be $\Xi_b^{(0,-)}\pi$ and for the heavier one $\Xi_b^{*(0,-)}\pi$. The lighter $\Xi_b(1P, 1/2)^-$ state could not be observed as it would likely decay primarily through the intermediate Ξ_b^0 resonance which is below threshold to decay to $\Xi_b^-\pi^+$. However, hints of such $\Xi_b(1P, 1/2)^- \rightarrow \Xi_b^0(\Xi_b^0\pi^0)\pi^-$ decay are observed in the $\Xi_b^0\pi^-$ spectrum as a partially reconstructed feed-down component.

Acknowledgements

We express our gratitude to our colleagues in the CERN accelerator departments for the excellent performance of the LHC. We thank the technical and administrative staff at the LHCb institutes. We acknowledge support from CERN and from the national agencies: CAPES, CNPq, FAPERJ and FINEP (Brazil); MOST and NSFC (China); CNRS/IN2P3 (France); BMBF, DFG and MPG (Germany); INFN (Italy); NWO (Netherlands); MNiSW and NCN (Poland); MCID/IFA (Romania); MICINN (Spain); SNSF and SER (Switzerland); NASU (Ukraine); STFC (United Kingdom); DOE NP and NSF (USA). We acknowledge the computing resources that are provided by CERN, IN2P3 (France), KIT and DESY (Germany), INFN (Italy), SURF (Netherlands), PIC (Spain),

GridPP (United Kingdom), CSCS (Switzerland), IFIN-HH (Romania), CBPF (Brazil), Polish WLCG (Poland) and NERSC (USA). We are indebted to the communities behind the multiple open-source software packages on which we depend. Individual groups or members have received support from ARC and ARDC (Australia); Minciencias (Colombia); AvH Foundation (Germany); EPLANET, Marie Skłodowska-Curie Actions, ERC and NextGenerationEU (European Union); A*MIDEX, ANR, IPhU and Labex P2IO, and Région Auvergne-Rhône-Alpes (France); Key Research Program of Frontier Sciences of CAS, CAS PIFI, CAS CCEPP, Fundamental Research Funds for the Central Universities, and Sci. & Tech. Program of Guangzhou (China); GVA, XuntaGal, GENCAT, Inditex, InTalent and Prog. Atracción Talento, CM (Spain); SRC (Sweden); the Leverhulme Trust, the Royal Society and UKRI (United Kingdom).

References

- [1] M. Gell-Mann, *A schematic model of baryons and mesons*, Phys. Lett. **8** (1964) 214.
- [2] G. Zweig, *An SU_3 model for strong interaction symmetry and its breaking; Version 1* CERN-TH-401, CERN, Geneva, 1964.
- [3] E. Klempt and J.-M. Richard, *Baryon spectroscopy*, Rev. Mod. Phys. **82** (2010) 1095, [arXiv:0901.2055](#).
- [4] CDF Collaboration, T. Aaltonen *et al.*, *Observation and mass measurement of the baryon Ξ_b^-* , Phys. Rev. Lett. **99** (2007) 052002.
- [5] CDF collaboration, T. Aaltonen *et al.*, *Observation of the Ξ_b^0 baryon*, Phys. Rev. Lett. **107** (2011) 102001, [arXiv:1107.4015](#).
- [6] CMS collaboration, S. Chatrchyan *et al.*, *Observation of a new Ξ_b baryon*, Phys. Rev. Lett. **108** (2012) 252002, [arXiv:1204.5955](#).
- [7] LHCb collaboration, R. Aaij *et al.*, *Observation of two new Ξ_b^- baryon resonances*, Phys. Rev. Lett. **114** (2015) 062004, [arXiv:1411.4849](#).
- [8] LHCb collaboration, R. Aaij *et al.*, *First branching fraction measurement of the suppressed decay $\Xi_c^0 \rightarrow \pi^- \Lambda_c^+$* , Phys. Rev. **D102** (2020) 071101(R), [arXiv:2007.12096](#).
- [9] K.-L. Wang, Y.-X. Yao, X.-H. Zhong, and Q. Zhao, *Strong and radiative decays of the low-lying S- and P-wave singly heavy baryons*, Phys. Rev. **D96** (2017) 116016.
- [10] B. Chen, K.-W. Wei, X. Liu, and A. Zhang, *Role of newly discovered $\Xi_b(6227)^-$ for constructing excited bottom baryon family*, Phys. Rev. **D98** (2018) 031502.
- [11] Y. Kawakami and M. Harada, *Singly heavy baryons with chiral partner structure in a three-flavor chiral model*, Phys. Rev. **D99** (2019) 094016.
- [12] Y. Kim, Y.-R. Liu, M. Oka, and K. Suzuki, *Heavy baryon spectrum with chiral multiplets of scalar and vector diquarks*, Phys. Rev. **D104** (2021) 054012.
- [13] H.-Z. He, W. Liang, Q.-F. Lü, and Y.-B. Dong, *Strong decays of the low-lying bottom strange baryons*, Science China Physics, Mechanics and Astronomy **64** (2021) .

- [14] A. J. Arifi, D. Suenaga, and A. Hosaka, *Relativistic corrections to decays of heavy baryons in the quark model*, Phys. Rev. **D103** (2021) 094003.
- [15] B. Chen, K.-W. Wei, and A. Zhang, *Assignments of Λ_Q and Ξ_Q baryons in the heavy quark-light diquark picture*, Eur. Phys. J. **A51** (2015) 82, [arXiv:1406.6561](#).
- [16] D. Ebert, R. N. Faustov, and V. O. Galkin, *Spectroscopy and Regge trajectories of heavy baryons in the relativistic quark-diquark picture*, Phys. Rev. **D84** (2011) 014025.
- [17] W. Roberts and M. Pervin, *Heavy baryons in a quark model*, Int. J. Mod. Phys. **A23** (2008) 2817, [arXiv:0711.2492](#).
- [18] CMS collaboration, A. M. Sirunyan *et al.*, *Observation of a new excited beauty strange Baryon Decaying to $\Xi_b^- \pi^+ \pi^-$* , Phys. Rev. Lett. **126** (2021) 252003.
- [19] LHCb collaboration, A. A. Alves Jr. *et al.*, *The LHCb detector at the LHC*, JINST **3** (2008) S08005.
- [20] LHCb collaboration, R. Aaij *et al.*, *LHCb detector performance*, Int. J. Mod. Phys. **A30** (2015) 1530022, [arXiv:1412.6352](#).
- [21] R. Aaij *et al.*, *Performance of the LHCb Vertex Locator*, JINST **9** (2014) P09007, [arXiv:1405.7808](#).
- [22] R. Arink *et al.*, *Performance of the LHCb Outer Tracker*, JINST **9** (2014) P01002, [arXiv:1311.3893](#).
- [23] P. d'Argent *et al.*, *Improved performance of the LHCb Outer Tracker in LHC Run 2*, JINST **12** (2017) P11016, [arXiv:1708.00819](#).
- [24] M. Adinolfi *et al.*, *Performance of the LHCb RICH detector at the LHC*, Eur. Phys. J. **C73** (2013) 2431, [arXiv:1211.6759](#).
- [25] T. Sjöstrand, S. Mrenna, and P. Skands, *A brief introduction to PYTHIA 8.1*, Comput. Phys. Commun. **178** (2008) 852, [arXiv:0710.3820](#).
- [26] I. Belyaev *et al.*, *Handling of the generation of primary events in Gauss, the LHCb simulation framework*, J. Phys. Conf. Ser. **331** (2011) 032047.
- [27] D. J. Lange, *The EvtGen particle decay simulation package*, Nucl. Instrum. Meth. **A462** (2001) 152.
- [28] Geant4 collaboration, J. Allison *et al.*, *Geant4 developments and applications*, IEEE Trans. Nucl. Sci. **53** (2006) 270.
- [29] M. Clemencic *et al.*, *The LHCb Simulation Application, Gauss: Design, Evolution and Experience*, J. Phys. Conf. Ser. **331** (2011) 032023.
- [30] Particle Data Group, R. L. Workman *et al.*, *Review of particle physics*, Prog. Theor. Exp. Phys. **2022** (2022) 083C01.
- [31] M. De Cian, S. Farry, P. Seyfert, and S. Stahl, *Fast neural-net based fake track rejection in the LHCb reconstruction*, LHCb-PUB-2017-011, 2017.

- [32] R. Aaij *et al.*, *Selection and processing of calibration samples to measure the particle identification performance of the LHCb experiment in Run 2*, Eur. Phys. J. Tech. Instr. **6** (2019) 1, [arXiv:1803.00824](#).
- [33] B. P. Roe *et al.*, *Boosted decision trees as an alternative to artificial neural networks for particle identification*, Nucl. Instrum. Meth. **543** (2005) 577.
- [34] *See Supplemental Material at [URL will be inserted by publisher] for further details, .*
- [35] LHCb collaboration, R. Aaij *et al.*, *First observation of excited Ω_b^- states*, Phys. Rev. Lett. **124** (2020) 082002, [arXiv:2001.00851](#).
- [36] W. D. Hulsbergen, *Decay chain fitting with a Kalman filter*, Nucl. Instrum. Meth. **A552** (2005) 566, [arXiv:physics/0503191](#).
- [37] J. D. Jackson, *Remarks on the phenomenological analysis of resonances*, Nuovo Cim. **34** (1964) 1644–1666.
- [38] J. M. Blatt and V. F. Weisskopf, *Theoretical nuclear physics*, Springer, New York, 1952.
- [39] T. Skwarnicki, *A study of the radiative cascade transitions between the Upsilon-prime and Upsilon resonances*, PhD thesis, Institute of Nuclear Physics, Krakow, 1986, DESY-F31-86-02.
- [40] LHCb collaboration, R. Aaij *et al.*, *Precision measurement of D meson mass differences*, JHEP **06** (2013) 065, [arXiv:1304.6865](#).
- [41] LHCb collaboration, R. Aaij *et al.*, *Observation of two new Ξ_b^- baryon resonances*, Phys. Rev. Lett. **114** (2015) 062004, [arXiv:1411.4849](#).
- [42] LHCb collaboration, R. Aaij *et al.*, *Observation of five new narrow Ω_c^0 states decaying to $\Xi_c^+ K^-$* , Phys. Rev. Lett. **118** (2017) 182001, [arXiv:1703.04639](#).
- [43] LHCb collaboration, R. Aaij *et al.*, *Observation of a new Ξ_b^- resonance*, Phys. Rev. Lett. **121** (2018) 072002, [arXiv:1805.09418](#).
- [44] LHCb collaboration, R. Aaij *et al.*, *Observation of two resonances in the $\Lambda_b^0 \pi^\pm$ systems and precise measurement of Σ_b^\pm and $\Sigma_b^{*\pm}$ properties*, Phys. Rev. Lett. **122** (2019) 012001, [arXiv:1809.07752](#).

Supplemental material

Figure 3 shows the mass distributions of the selected Ξ_b^- and Ξ_b^0 signal candidates. These distributions are fitted with an asymmetric Gaussian-like function with power-law tails for the signal component, an exponential function for the combinatorial background and an empirical function for partially reconstructed backgrounds. The fitted signal yields are $12\,020 \pm 140$ for $\Xi_b^- \rightarrow \Xi_c^0 \pi^-$, $27\,300 \pm 210$ for $\Xi_b^0 \rightarrow \Xi_c^+ \pi^-$, $5\,680 \pm 100$ for $\Xi_b^- \rightarrow \Xi_c^0 \pi^- \pi^+ \pi^-$, $11\,690 \pm 180$ for $\Xi_b^0 \rightarrow \Xi_c^+ \pi^- \pi^+ \pi^-$ decays.

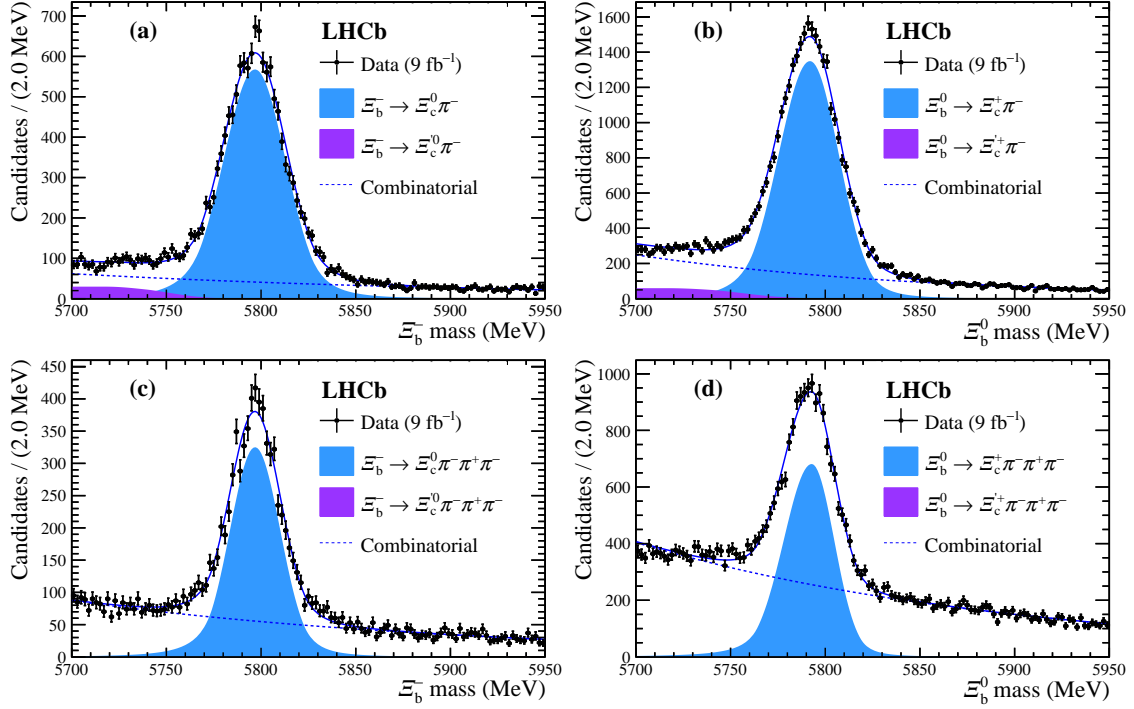


Figure 3: Mass distributions of the (a) $\Xi_b^- \rightarrow \Xi_c^0 \pi^-$, (b) $\Xi_b^0 \rightarrow \Xi_c^+ \pi^-$, (c) $\Xi_b^- \rightarrow \Xi_c^0 \pi^- \pi^+ \pi^-$ and (d) $\Xi_b^0 \rightarrow \Xi_c^+ \pi^- \pi^+ \pi^-$ selected signal candidates.

Figures 4 and 5 show the mass-difference ($Q = m_{\Xi_b \pi \pi} - m_{\Xi_b} - 2m_\pi$) distributions inside and outside the mass windows corresponding to the known $\Xi_b \pi$ intermediate resonances. Simultaneous fits are performed using the fit models presented in the Letter, with the resonance parameters fixed to their nominal values. Yields are allowed to vary in the fit. The observed suppression of decays not proceeding through the respective intermediate resonances confirms the decay pattern described in the text.

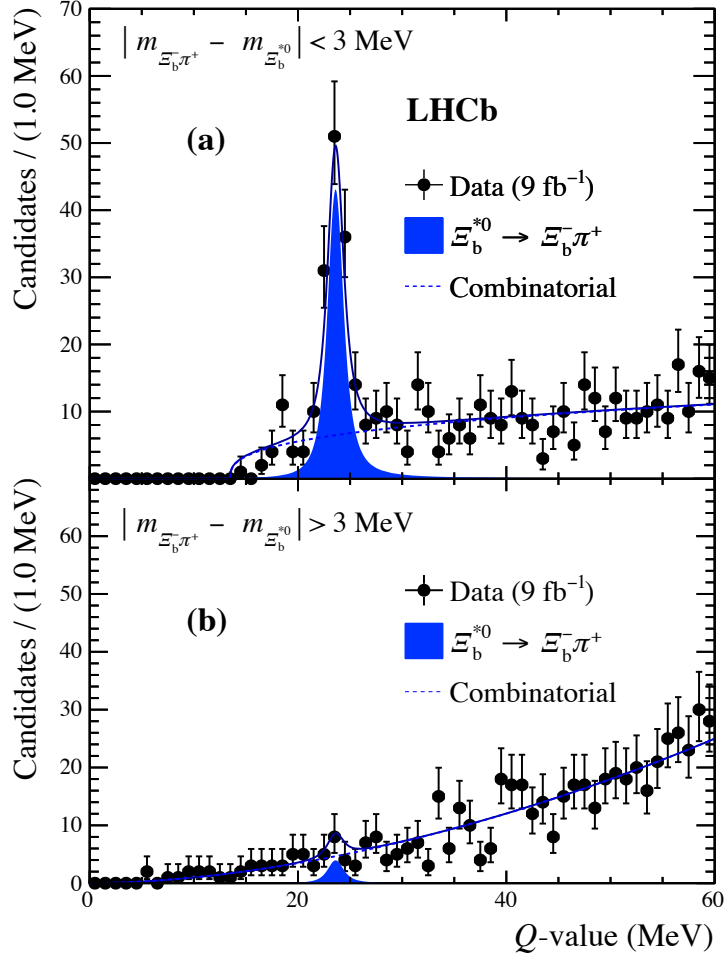


Figure 4: Distributions of the mass difference $Q = m_{\Xi_b^- \pi^+ \pi^-} - m_{\Xi_b^-} - 2m_\pi$ for selected $\Xi_b^- \pi^+ \pi^-$ candidates, (a) in the Ξ_b^{*0} mass window and (b) outside the Ξ_b^{*0} mass window. The results of the simultaneous fit are superimposed.

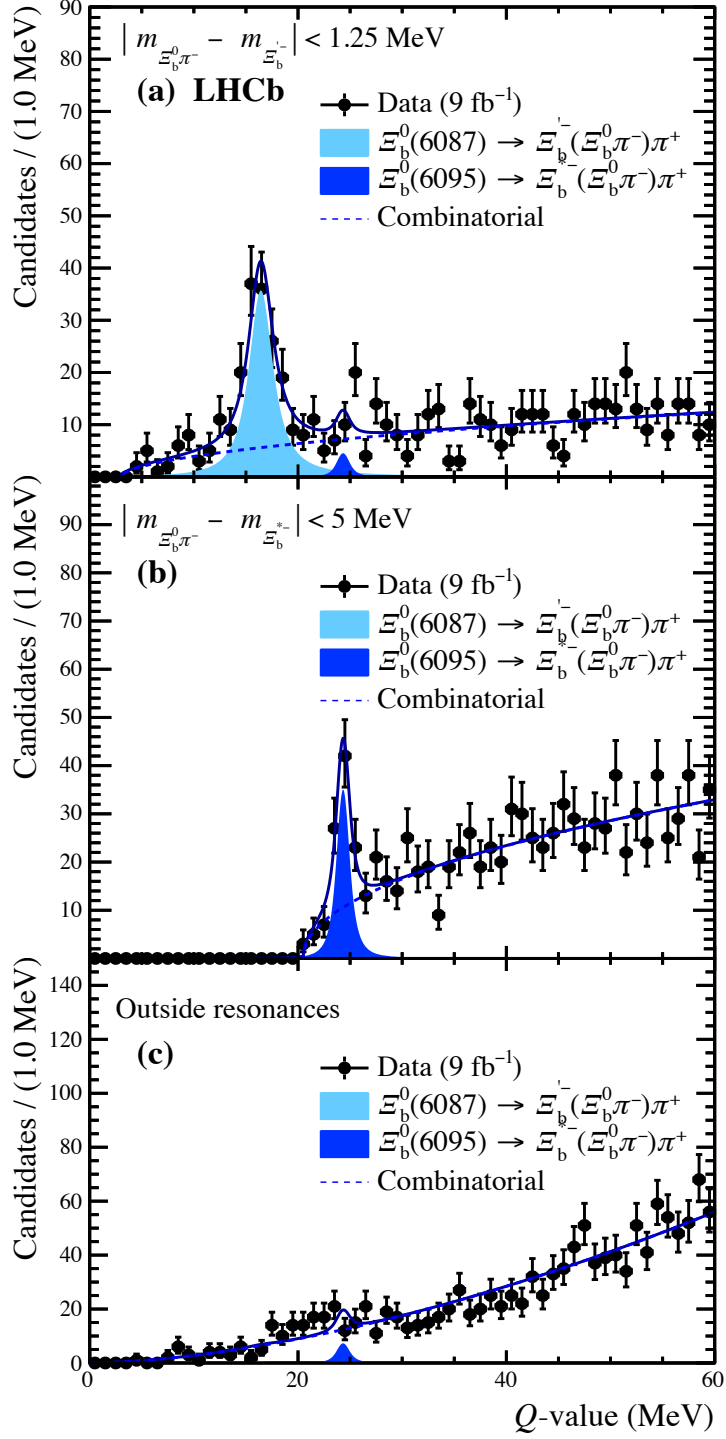


Figure 5: Distributions of the mass difference $Q = m_{\Xi_b^0 \pi^+ \pi^-} - m_{\Xi_b} - 2m_\pi$ for selected $\Xi_b^0 \pi^+ \pi^-$ candidates, (a) in the $\Xi_b'^-$ mass window, (b) in the Ξ_b^{*-} mass window and (c) outside the mass windows of the intermediate resonances. The results of the simultaneous fit are superimposed.

LHCb collaboration

R. Aaij³², A.S.W. Abdelmotteleb⁵¹, C. Abellan Beteta⁴⁵, F. Abudinén⁵¹,
T. Ackernley⁵⁵, B. Adeva⁴¹, M. Adinolfi⁴⁹, P. Adlarson⁷⁷, H. Afsharnia⁹,
C. Agapopoulou⁴³, C.A. Aidala⁷⁸, Z. Ajaltouni⁹, S. Akar⁶⁰, K. Akiba³²,
P. Albicocco²³, J. Albrecht¹⁵, F. Alessio⁴³, M. Alexander⁵⁴, A. Alfonso Alberro⁴⁰,
Z. Aliouche⁵⁷, P. Alvarez Cartelle⁵⁰, R. Amalric¹³, S. Amato², J.L. Amey⁴⁹,
Y. Amhis^{11,43}, L. An⁵, L. Anderlini²², M. Andersson⁴⁵, A. Andreianov³⁸,
M. Andreotti²¹, D. Andreou⁶³, D. Ao⁶, F. Archilli^{31,t}, A. Artamonov³⁸,
M. Artuso⁶³, E. Aslanides¹⁰, M. Atzeni⁴⁵, B. Audurier¹², I. Bachiller Perea⁸,
S. Bachmann¹⁷, M. Bachmayer⁴⁴, J.J. Back⁵¹, A. Bailly-reyre¹³,
P. Baladron Rodriguez⁴¹, V. Balagura¹², W. Baldini^{21,43}, J. Baptista de Souza Leite¹,
M. Barbeti^{22,k}, I. R. Barbosa⁶⁵, R.J. Barlow⁵⁷, S. Barsuk¹¹, W. Barter⁵³,
M. Bartolini⁵⁰, F. Baryshnikov³⁸, J.M. Basels¹⁴, G. Bassi^{29,q}, B. Batsukh⁴,
A. Battig¹⁵, A. Bay⁴⁴, A. Beck⁵¹, M. Becker¹⁵, F. Bedeschi²⁹, I.B. Bediaga¹,
A. Beiter⁶³, S. Belin⁴¹, V. Bellee⁴⁵, K. Belous³⁸, I. Belov²⁴, I. Belyaev³⁸,
G. Benane¹⁰, G. Bencivenni²³, E. Ben-Haim¹³, A. Bereznoy³⁸, R. Bernet⁴⁵,
S. Bernet Andres³⁹, D. Berninghoff¹⁷, H.C. Bernstein⁶³, C. Bertella⁵⁷, A. Bertolin²⁸,
C. Betancourt⁴⁵, F. Betti⁴³, Ia. Bezshyiko⁴⁵, J. Bhom³⁵, L. Bian⁶⁹,
M.S. Bieker¹⁵, N.V. Biesuz²¹, P. Billoir¹³, A. Biolchini³², M. Birch⁵⁶,
F.C.R. Bishop⁵⁰, A. Bitadze⁵⁷, A. Bizzeti⁴³, M.P. Blago⁵⁰, T. Blake⁵¹, F. Blanc⁴⁴,
J.E. Blank¹⁵, S. Blusk⁶³, D. Bobulska⁵⁴, V. Bocharnikov³⁸, J.A. Boelhauve¹⁵,
O. Boente Garcia¹², T. Boettcher⁶⁰, A. Boldyrev³⁸, C.S. Bolognani⁷⁵,
R. Bolzonella^{21,j}, N. Bondar³⁸, F. Borgato^{28,43}, S. Borghi⁵⁷, M. Borsato¹⁷,
J.T. Borsuk³⁵, S.A. Bouchiba⁴⁴, T.J.V. Bowcock⁵⁵, A. Boyer⁴³, C. Bozzi²¹,
M.J. Bradley⁵⁶, S. Braun⁶¹, A. Brea Rodriguez⁴¹, N. Breer¹⁵, J. Brodzicka³⁵,
A. Brossa Gonzalo⁴¹, J. Brown⁵⁵, D. Brundu²⁷, A. Buonauro⁴⁵, L. Buonincontri²⁸,
A.T. Burke⁵⁷, C. Burr⁴³, A. Bursche⁶⁷, A. Butkevich³⁸, J.S. Butter³²,
J. Buytaert⁴³, W. Byczynski⁴³, S. Cadeddu²⁷, H. Cai⁶⁹, R. Calabrese^{21,j},
L. Calefice¹⁵, S. Cali²³, M. Calvi^{26,n}, M. Calvo Gomez³⁹, P. Campana²³,
D.H. Campora Perez⁷⁵, A.F. Campoverde Quezada⁶, S. Capelli^{26,n}, L. Capriotti²¹,
A. Carbone^{20,h}, R. Cardinale^{24,l}, A. Cardini²⁷, P. Carniti^{26,n}, L. Carus¹⁷,
A. Casais Vidal⁴¹, R. Caspary¹⁷, G. Casse⁵⁵, M. Cattaneo⁴³, G. Cavallero²¹,
V. Cavallini^{21,j}, S. Celani⁴⁴, J. Cerasoli¹⁰, D. Cervenkov⁵⁸, A.J. Chadwick⁵⁵,
I. Chahrouh⁷⁸, M.G. Chapman⁴⁹, M. Charles¹³, Ph. Charpentier⁴³,
C.A. Chavez Barajas⁵⁵, M. Chefdeville⁸, C. Chen¹⁰, S. Chen⁴, A. Chernov³⁵,
S. Chernyshenko⁴⁷, V. Chobanova^{41,w}, S. Cholak⁴⁴, M. Chruszcz³⁵,
A. Chubykin³⁸, V. Chulikov³⁸, P. Ciambone²³, M.F. Cicala⁵¹, X. Cid Vidal⁴¹,
G. Ciezarek⁴³, P. Cifra⁴³, G. Ciullo^{j,21}, P.E.L. Clarke⁵³, M. Clemencic⁴³,
H.V. Cliff⁵⁰, J. Closier⁴³, J.L. Cobbedick⁵⁷, V. Coco⁴³, J. Cogan¹⁰,
E. Cogneras⁹, L. Cojocariu³⁷, P. Collins⁴³, T. Colombo⁴³, A. Comerma-Montells⁴⁰,
L. Congedo¹⁹, A. Contu²⁷, N. Cooke⁵⁴, I. Corredoira⁴¹, G. Corti⁴³,
B. Couturier⁴³, D.C. Craik⁴⁵, M. Cruz Torres^{1,f}, R. Currie⁵³, C.L. Da Silva⁶²,
S. Dadabaev³⁸, L. Dai⁶⁶, X. Dai⁵, E. Dall’Oco¹⁵, J. Dalseno⁴¹,
C. D’Ambrosio⁴³, J. Daniel⁹, A. Danilina³⁸, P. d’Argent¹⁹, J.E. Davies⁵⁷,
A. Davis⁵⁷, O. De Aguiar Francisco⁵⁷, J. de Boer³², K. De Bruyn⁷⁴, S. De Capua⁵⁷,
M. De Cian¹⁷, U. De Freitas Carneiro Da Graça¹, E. De Lucia²³, J.M. De Miranda¹,
L. De Paula², M. De Serio^{19,g}, D. De Simone⁴⁵, P. De Simone²³, F. De Vellis¹⁵,
J.A. de Vries⁷⁵, C.T. Dean⁶², F. Debernardis^{19,g}, D. Decamp⁸, V. Dedu¹⁰,
L. Del Buono¹³, B. Delaney⁵⁹, H.-P. Dembinski¹⁵, V. Denysenko⁴⁵, O. Deschamps⁹,

- ³⁹ *DS4DS, La Salle, Universitat Ramon Llull, Barcelona, Spain*
- ⁴⁰ *ICCUB, Universitat de Barcelona, Barcelona, Spain*
- ⁴¹ *Instituto Galego de Física de Altas Enerxías (IGFAE), Universidade de Santiago de Compostela, Santiago de Compostela, Spain*
- ⁴² *Instituto de Física Corpuscular, Centro Mixto Universidad de Valencia - CSIC, Valencia, Spain*
- ⁴³ *European Organization for Nuclear Research (CERN), Geneva, Switzerland*
- ⁴⁴ *Institute of Physics, Ecole Polytechnique Fédérale de Lausanne (EPFL), Lausanne, Switzerland*
- ⁴⁵ *Physik-Institut, Universität Zürich, Zürich, Switzerland*
- ⁴⁶ *NSC Kharkiv Institute of Physics and Technology (NSC KIPT), Kharkiv, Ukraine*
- ⁴⁷ *Institute for Nuclear Research of the National Academy of Sciences (KINR), Kyiv, Ukraine*
- ⁴⁸ *University of Birmingham, Birmingham, United Kingdom*
- ⁴⁹ *H.H. Wills Physics Laboratory, University of Bristol, Bristol, United Kingdom*
- ⁵⁰ *Cavendish Laboratory, University of Cambridge, Cambridge, United Kingdom*
- ⁵¹ *Department of Physics, University of Warwick, Coventry, United Kingdom*
- ⁵² *STFC Rutherford Appleton Laboratory, Didcot, United Kingdom*
- ⁵³ *School of Physics and Astronomy, University of Edinburgh, Edinburgh, United Kingdom*
- ⁵⁴ *School of Physics and Astronomy, University of Glasgow, Glasgow, United Kingdom*
- ⁵⁵ *Oliver Lodge Laboratory, University of Liverpool, Liverpool, United Kingdom*
- ⁵⁶ *Imperial College London, London, United Kingdom*
- ⁵⁷ *Department of Physics and Astronomy, University of Manchester, Manchester, United Kingdom*
- ⁵⁸ *Department of Physics, University of Oxford, Oxford, United Kingdom*
- ⁵⁹ *Massachusetts Institute of Technology, Cambridge, MA, United States*
- ⁶⁰ *University of Cincinnati, Cincinnati, OH, United States*
- ⁶¹ *University of Maryland, College Park, MD, United States*
- ⁶² *Los Alamos National Laboratory (LANL), Los Alamos, NM, United States*
- ⁶³ *Syracuse University, Syracuse, NY, United States*
- ⁶⁴ *School of Physics and Astronomy, Monash University, Melbourne, Australia, associated to ⁵¹*
- ⁶⁵ *Pontifícia Universidade Católica do Rio de Janeiro (PUC-Rio), Rio de Janeiro, Brazil, associated to ²*
- ⁶⁶ *Physics and Micro Electronic College, Hunan University, Changsha City, China, associated to ⁷*
- ⁶⁷ *Guangdong Provincial Key Laboratory of Nuclear Science, Guangdong-Hong Kong Joint Laboratory of Quantum Matter, Institute of Quantum Matter, South China Normal University, Guangzhou, China, associated to ³*
- ⁶⁸ *Lanzhou University, Lanzhou, China, associated to ⁴*
- ⁶⁹ *School of Physics and Technology, Wuhan University, Wuhan, China, associated to ³*
- ⁷⁰ *Departamento de Física, Universidad Nacional de Colombia, Bogota, Colombia, associated to ¹³*
- ⁷¹ *Universität Bonn - Helmholtz-Institut für Strahlen und Kernphysik, Bonn, Germany, associated to ¹⁷*
- ⁷² *Eotvos Lorand University, Budapest, Hungary, associated to ⁴³*
- ⁷³ *INFN Sezione di Perugia, Perugia, Italy, associated to ²¹*
- ⁷⁴ *Van Swinderen Institute, University of Groningen, Groningen, Netherlands, associated to ³²*
- ⁷⁵ *Universiteit Maastricht, Maastricht, Netherlands, associated to ³²*
- ⁷⁶ *Tadeusz Kosciuszko Cracow University of Technology, Cracow, Poland, associated to ³⁵*
- ⁷⁷ *Department of Physics and Astronomy, Uppsala University, Uppsala, Sweden, associated to ⁵⁴*
- ⁷⁸ *University of Michigan, Ann Arbor, MI, United States, associated to ⁶³*

^a *Universidade de Brasília, Brasília, Brazil*

^b *Universidade Federal do Triângulo Mineiro (UFMT), Uberaba-MG, Brazil*

^c *Central South U., Changsha, China*

^d *Hangzhou Institute for Advanced Study, UCAS, Hangzhou, China*

^e *Excellence Cluster ORIGINS, Munich, Germany*

^f *Universidad Nacional Autónoma de Honduras, Tegucigalpa, Honduras*

^g *Università di Bari, Bari, Italy*

^h *Università di Bologna, Bologna, Italy*

ⁱ *Università di Cagliari, Cagliari, Italy*

^j *Università di Ferrara, Ferrara, Italy*

^k *Università di Firenze, Firenze, Italy*

^l *Università di Genova, Genova, Italy*

^m *Università degli Studi di Milano, Milano, Italy*

ⁿ *Università di Milano Bicocca, Milano, Italy*

^o *Università di Padova, Padova, Italy*

^p *Università di Perugia, Perugia, Italy*

^q *Scuola Normale Superiore, Pisa, Italy*

^r *Università di Pisa, Pisa, Italy*

^s *Università della Basilicata, Potenza, Italy*

^t *Università di Roma Tor Vergata, Roma, Italy*

^u *Università di Urbino, Urbino, Italy*

^v *Universidad de Alcalá, Alcalá de Henares, Spain*

^w *Universidade da Coruña, Coruña, Spain*

[†] *Deceased*